Rev. Roum. Sci. Techn.– Électrotechn. et Énerg.
Vol. **71**, *1*, pp. 71–76, Bucarest, 2026

PHOTOVOLTAIC FLUCTUATION SMOOTHING: MULTI-CRITERION OPTIMIZATION OF LOW-PASS FILTERS

SALIHA BOULAHCHICHE, ISMAIL BENDAAS, SMAIL SEMAOUI, KADA BOUCHOUICHA, ABDELHAK RAZAGUI, AMAR HADJ ARAB, KAMEL ABDELADIM

Keywords: Photovoltaic (PV) smoothing; Low-pass filter; Battery degradation; Ramp rate control; Grid integration; Multi-criteria analysis.

The integration of photovoltaic (PV) systems into power grids faces inherent challenges posed by power fluctuations driven by variable weather conditions, potentially destabilizing grid operations. This study, based on real data from the CDER network in Algeria, proposes a systematic comparative analysis of a discrete first-order low-pass filter (LPF) for attenuating these fluctuations by evaluating three representative time constants (TC = 10, 20, 30 min). Using a novel multi-criteria evaluation framework, we assess both smoothing performance and battery stress effects, and introduce an innovative SVM-based heatmap classification method for ramp rate (RR %) pattern analysis. Key findings reveal fundamental trade-offs: while TC = 30 min achieves an 80% reduction in high fluctuations (RR% > 10%), it concurrently increases battery energy throughput by 35%, potentially accelerating long-term degradation. The TC = 20 min configuration emerges as the optimal balance, delivering 60% power variance reduction while limiting the mean squared error (MSE) increase to just 8%. Our results provide: (1) quantitative evidence for LPF parameter optimization, (2) visual analytics for fluctuation pattern recognition, and (3) practical guidelines for maintaining grid stability while extending battery lifespan in PV-integrated systems.

1. INTRODUCTION

The integration of photovoltaic (PV) systems into modern electrical grids faces a major challenge due to the intrinsic variability of solar energy production [1–11]. Rapid power fluctuations, which can exceed 10% per minute because of cloud passage or atmospheric changes, compromise grid stability and may lead to non-compliance with energy quality standards, such as those defined by the International Electrotechnical Commission (IEC 61727) [3–5]. These variations also cause critical frequency deviations and increase the demand on battery energy storage systems (BESS), accelerating their degradation.

Various smoothing techniques have been proposed to mitigate these effects. Traditional methods, such as simple and exponential moving averages (EMA), reduce short-term fluctuations but generally fail to address battery cycling or long-term stability. Kalman and adaptive filters offer dynamic tracking of power variations but require accurate system models and complex implementation. Fourier- or wavelet-based methods analyze fluctuations in the frequency domain but are rarely applied to operational battery management. Most existing studies focus on a single performance metric and do not provide an integrated assessment of smoothing performance, battery cycling, and state-of-charge (SoC) evolution.

This study presents a systematic analysis of a discrete low-pass filter (LPF) applied to real operational data from the CDER PV network. It investigates how the LPF time constant affects ramp rate mitigation and variance reduction, examines its impact on battery charge/discharge behavior and SoC evolution, and seeks to identify an optimal trade-off between grid stability and battery preservation. A multi-criteria methodology is introduced that simultaneously evaluates smoothing performance, classification of battery operating states using support vector machines (SVMs), and SoC dynamics [1,2,4,6,9,10]. Analyses of three time constants (10, 20, and 30 min) provide practical guidance for PV system operation.

The results show that a 20 min time constant offers the best compromise, reducing power fluctuations by approximately 60% while limiting battery energy exchanges to under 15%. This integrated approach establishes quantitative relationships between LPF parameters, grid stability, and battery constraints, offering valuable guidance for network operators and PV managers. The paper is organized as follows: Section 2 describes the PV–BESS configuration, Section 3 addresses issues from intermittent power sources, Section 4 details the methodology, Section 5 presents the SVM-based optimization, Section 6 discusses results, and Section 7 concludes with final remarks and future directions

2. CONFIGURATION OF THE PV-BESS SYSTEM FOR POWER SMOOTHING

This diagram represents a hybrid architecture combining a photovoltaic (PV) system and a battery energy storage system (BESS), designed to mitigate fluctuations in the produced power. Solar irradiation is converted into direct current electrical power (Ppv) by the PV panels, then processed on the direct current side via an inverter. The BESS, combined with a smoothing strategy — such as a low-pass filter — intervenes by absorbing or delivering energy to stabilize the delivered power. This regulated power is then converted into alternating current (AC) before being injected into the electrical grid (PG).

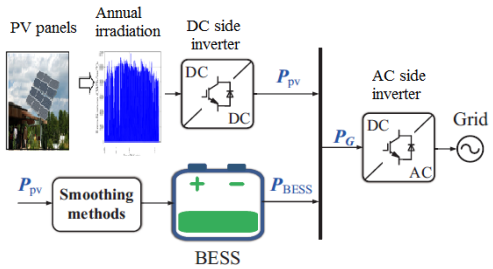

Fig. 1 –PV-BESS design for power fluctuation mitigation.

3. PROBLEMS WITH AN INTERMITTENT POWER SOURCE

Before detailing the smoothing solution, it is crucial to quantify the problems caused by PV intermittency. This section characterizes the power quality issues (flicker harmonics) that our proposed LPF aims to mitigate. The

Centre de Développement des Énergies Renouvelables (CDER), B.P. 62, Route de l'observatoire, Bouzareah, 16340 Alger, Algérie.
Emails: boulahchiche21@live.com, I.bendaas@cder.dz, s.semaoui@cder.dz, k.bouchouicha@cder.dz, a.razagui@cder.dz, a.hadjarab@cder.dz, arab@cder.dz, k.Abdeladim@cder.dz

DOI: 10.59277/RRST-EE.2026.1.12

following analysis demonstrates the direct impact of irradiance fluctuations on grid parameters, justifying the need for effective smoothing [4–6, 8].

3.1 EFFECT OF FLUCTUATIONS ON FLICKER LEVEL

Figure 2 shows that weather conditions directly influence the fluctuations of the current injected by the photovoltaic system, with stability in clear weather and abrupt variations in cloudy weather due to rapid changes in solar irradiance. These current fluctuations affect the voltage, as shown in Fig. 3, where flickers become significant on cloudy days due to sudden power variations, while they remain negligible on clear days and moderate on overcast days [2,3,5].

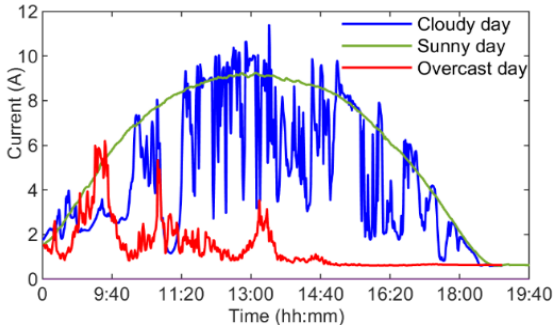

Fig. 2 – Current injected during a clear sky day, a cloudy day, and an overcast day.

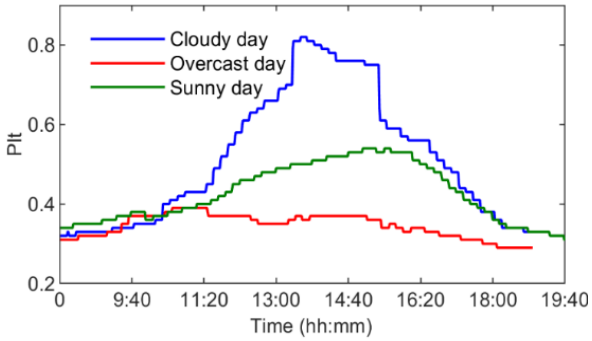

Fig. 3 – Plt flickers on a clear sky day, a cloudy day, and an overcast day.

3.2 EFFECT OF FLUCTUATIONS ON CURRENT AND VOLTAGE HARMONICS

Figures 4 and 5 demonstrate that PV power fluctuations, particularly pronounced on cloudy days, significantly degrade energy quality by increasing current and voltage harmonics, both at the inverter output and at the point of common coupling (PCC). In clear weather, where production is stable, the levels of total harmonic distortion (THD) remain low and within standards. On the other hand, the sudden power variations caused by the passage of clouds lead to a notable increase in harmonic distortions, more pronounced at the PCC than at the inverter [3,4,5,7,8].

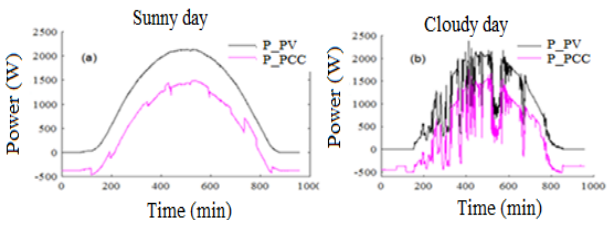

Fig. 4 – (a) Active power of the inverter and the PCC for a sunny day; (b) Active power of the inverter and the PCC for a cloudy day.

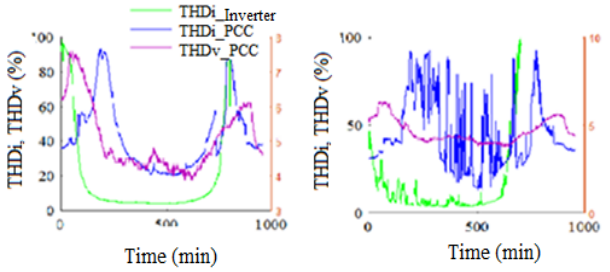

Fig. 5 – a) Power quality parameter of the inverter and the PCC for a sunny day; (b) Energy quality parameters of the inverter and the PCC for a cloudy day.

These results highlight the crucial importance of implementing appropriate filtering and smoothing solutions to improve energy quality parameters. Such an approach would effectively compensate for the harmful effects of solar intermittency, while ensuring the stability of the electrical grid and protecting sensitive equipment against harmonic disturbances. The following sections present a low-pass filter (LPF) methodology designed specifically to attenuate these rapid fluctuations, thereby mitigating the flicker and harmonic distortions characterized above.

4. METHODOLOGY

4.1 IMPLEMENTATION OF THE LOW-PASS FILTER

The discrete low-pass filter is modeled by its transfer function in the Z domain [9].

$$H(z) = \frac{\alpha}{1-(1-\alpha)z^{-1}}, \quad (1)$$

$$\alpha = \frac{\Delta t}{TC+\Delta t}, \quad (2)$$

where α is a smoothing coefficient (dimensionless); Δt is the Sampling time step (1 min in our study), and TC is a time constant (10, 20, or 30 min). This formulation allows for the attenuation of high frequencies (rapid fluctuations) while preserving the long-term trends of PV power.

4.2 BATTERY MODELING

The interaction between LPF and the storage system is described by [6]:

$$P_{SM} = P_{PV} \pm P_{BES}, \quad (3)$$

where P_{SM} represents the smoothed photovoltaic power or the reference power for smoothing; P_{PV} denotes the power produced by the photovoltaic system, and P_{BES} indicates the charging (absorbed) or discharging (injected) power by the energy storage system (ESS).

This fundamental equation illustrates how the storage system intervenes to compensate for fluctuations and provide stable power to the grid.

$$\mathrm{SoC}(t+1) = \mathrm{SoC}(t) - \frac{\mathrm{P_{BES}}(t)\cdot \mathrm{T}}{\mathrm{V(t)}\cdot 60 \cdot \mathrm{Q_{BESS}}} \cdot 100, \quad (4)$$

where the factor 60 converts the time step from minutes to hours, consistent with the battery capacity typically expressed in Ampere-hours (Ah); $\mathrm{P_{BES}}$ is the power exchanged by the battery (positive in charge, negative in discharge); T is the time constant (min); V(t) is the dynamic voltage; $\mathrm{Q_{BESS}}$ is the total battery capacity (Ah).

These coupled equations describe: (3) active smoothing through storage and (4) the evolution of the SoC. They allow for optimizing the trade-off between network stability and

battery preservation by quantifying the impact of LPF parameters.

4.3 CALCULATION OF MSE AND VARIANCE

The calculation of the MSE and the variance allows for the evaluation of two essential dimensions of the quality of filtering by an LPF. The MSE measures the average deviation between the smoothed signal and the original signal, reflecting the accuracy of the filtering. A high MSE value indicates a significant difference, which may suggest over-smoothing or an excessive time shift.

Variance, on the other hand, evaluates the dispersion of the remaining fluctuations after filtering. A significant reduction in variance indicates that rapid fluctuations have been effectively mitigated, which is crucial for the stability of the electrical grid. The corresponding formulas are [6]:

$$MSE = \frac{1}{n}\sum_{i=1}^{n}(y_i - y'_i)^2, \quad (5)$$

where y_i is the actual value; y'_i is the predicted value; n is the total number of observations

$$Variance = \frac{1}{n}\sum_{i=1}^{n}(x_i - x'_i)^2, \quad (6)$$

where x_i is the predicted value, x'_i is the mean of the predictive values, and n is the total number of observations.

4.4. SYSTEM SPECIFICATIONS AND DATA

The study area is located at the CDER test site in Algiers, Algeria (36.75°N, 3.05°E), situated in the northern coastal region of the country. Algiers features a hot-summer Mediterranean climate (Köppen classification: Csa), characterized by hot, dry summers and mild, wet winters. This climate zone experiences frequent cloud variability during transitional seasons, leading to significant short-term fluctuations in solar irradiance—making it a relevant environment for evaluating PV power smoothing strategies.

The study uses 1 min resolution power data from a 9.54 kWp grid-connected PV system at the CDER site, equipped with polycrystalline silicon modules tilted at 28° and facing south (azimuth = 0°). Data were acquired using a calibrated National Instruments data acquisition system, ensuring high-fidelity capture of rapid irradiance-driven transients essential for fluctuation analysis.

5. SVM-BASED CLASSIFICATION AND HEATMAP ANALYSIS FOR PV–BATTERY SYSTEM OPTIMIZATION

This study employs a Support Vector Machine (SVM) to jointly analyze photovoltaic power variability and battery operating states for different LPF time constants. Based on a set of normalized features describing battery power, its temporal variation, cumulative energy, and state of charge, the SVM classifies battery operation into charge, discharge, and stable modes using a nonlinear kernel. The resulting classifications are visualized through heatmaps, enabling an intuitive comparison of battery cycling behavior and state transitions across time constants. This combined SVM–heatmap approach provides an effective multi-criteria framework to assess the trade-off between PV fluctuation mitigation and battery stress reduction, and is implemented using MATLAB/Simulink

6. RESULTS AND DISCUSSION

The comparative analysis over a 20 min window, presented in Figure 6, demonstrates that the LPF method significantly reduces ramp events (40-50%) through effective smoothing, thereby minimizing battery power peaks and reducing stress on the storage system. Although this attenuation leads to a slight loss of accuracy in tracking PV power, LPF proves optimal for applications prioritizing grid stability and equipment preservation.

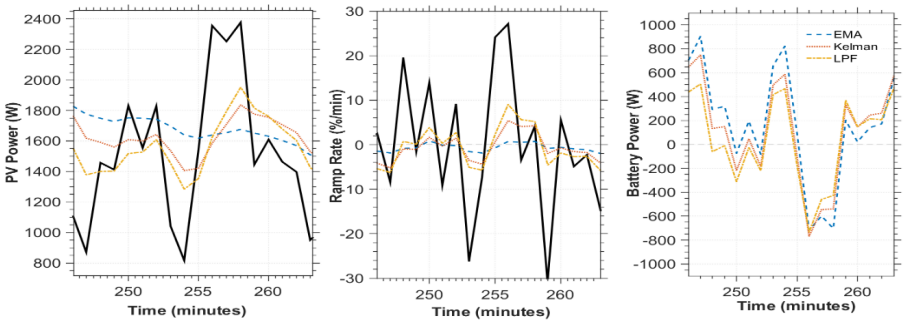

Fig. 6 – Smoothing methods.

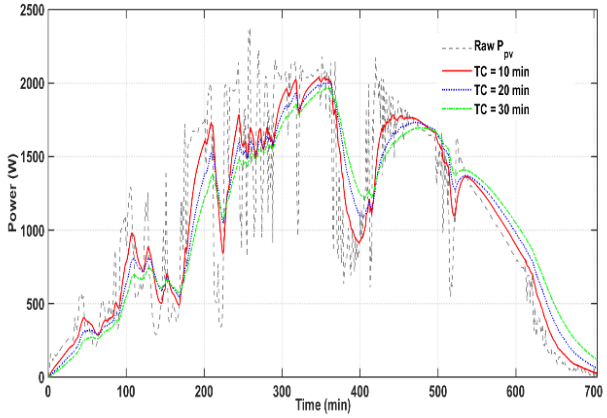

Fig. 7 – Comparison of Raw and Smoothed PV Power (LPF).

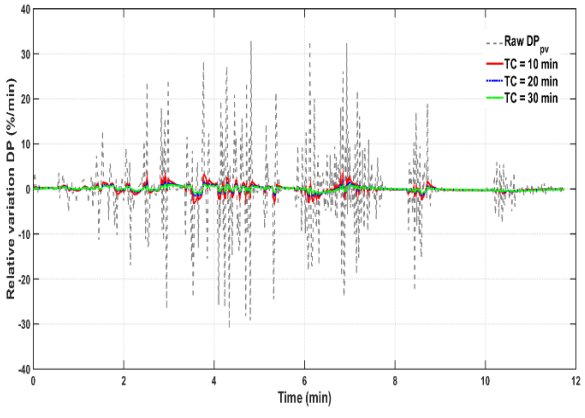

Fig. 8 – Relative Variation of PV Power (raw and smoothed).

Figure 7 clearly shows the effect of LPF filtering on PV power. The raw curve shows significant fluctuations (up to ±500 W), typical of solar variations. Filtering with TC = 10 min partially reduces these peaks while maintaining the overall dynamics. With TC = 20 min, the rapid fluctuations are significantly attenuated, while TC = 30 min produces a nearly smooth curve but introduces a noticeable delay of about 15-20 min during abrupt transitions.

Figure 8 reveals the impact on the instantaneous variation rates. The raw variations reach ±40%/min (with peaks at ±100%/min). Filtering gradually reduces these values: TC=10 min limits to ±15%/min, TC=20 min to ±10%/min, and TC=30 min to ±5%/min. It is observed that TC=20 min offers the best balance, sufficiently reducing variations while minimizing time lag.

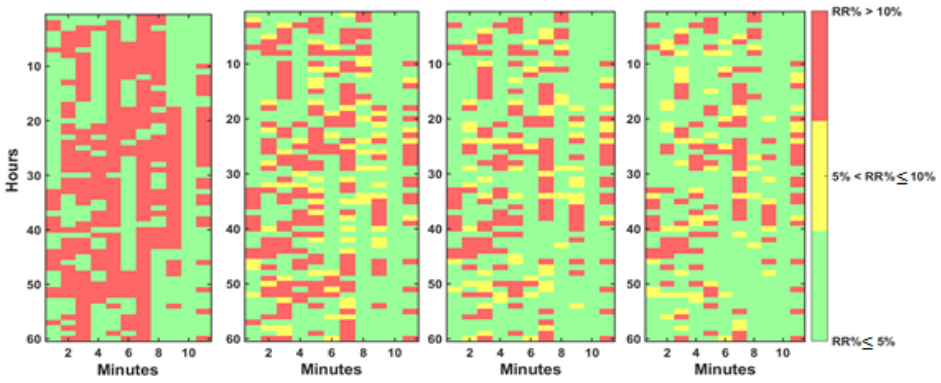

Fig. 9 – Heat maps for raw and TC

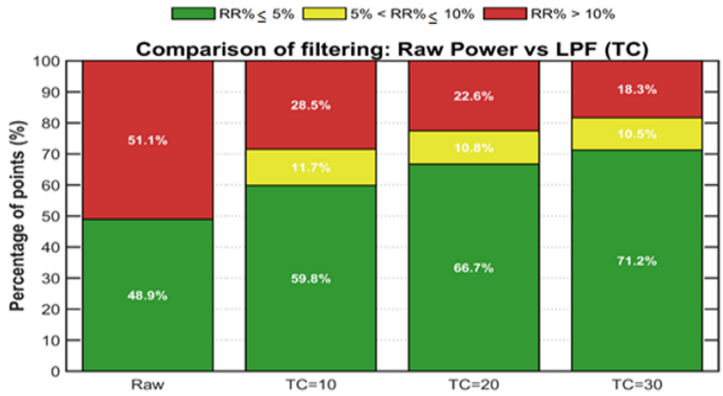

Fig. 10 – Heatmaps for raw comparison of raw vs filtered RR%.

Figures 9 and 10 show the heat map of the LPF filter on PV power variations. Without filtering, only 50% of the points have variations ≤5%, with 20% of peaks >10%. With TC = 10 min, the peaks >10% drop to 10%, and the variations ≤5% reach 60%. TC = 20 min provides the best balance: only 5% of peaks >10% and 75% of variations ≤ 5%. TC = 30 min eliminates almost all peaks (>10%) but causes over-smoothing (80% ≤ 5%). TC = 20 min remains the optimal choice.

The study demonstrates that the LPF filter with a TC of 20 min represents the optimal solution, effectively combining stability and responsiveness. While TC=10 min (response time: 23 min) shows high reactivity but insufficient smoothing, and TC = 30 min (response time: 67 min) provides excessive smoothing at the cost of significant delay, TC = 20 min (response time: 45 min) maintains a perfect balance. These rise time values, obtained through numerical simulation of the discrete filter's step response with linear interpolation between sampling points, are slightly higher than the theoretical approximation RT = 2.2 × TC due to discretization effects from the 1 min sampling step. This configuration significantly reduces critical fluctuations (>10%) while maintaining the essential dynamics of the photovoltaic signal. Table 1 illustrates the relationship between computation time (CT), response time (rise time), and the performance of the LPF in a photovoltaic system.

Table 1

Key trade-offs between time constants and response times

TC (min)	Rise Time (min)	Main Advantage	Major Drawback
10	23	High responsiveness	Insufficient smoothing
20	45	Optimal balance	—
30	67	Maximum smoothing	Critical delay

Figure 11 shows the joint evolution of variance and MSE as a function of the time constant (TC). It is clearly observed that when TC increases from 10 to 30 min, the variance of the filtered power decreases significantly (from 3.5 to 1 W²), indicating better stability. However, this improvement is accompanied by a gradual increase in the MSE (from 0.5 to 1.5 W²), indicating a loss of fidelity to the original signal. The remarkable point is at TC = 20 min, where the variance is halved (1.75 W²) while the MSE remains moderate (1 W²), confirming that this parameter offers the best compromise between stability and preservation of the photovoltaic signal characteristics. These quantitative results support the qualitative conclusions of the previous analyses.

Figure 11 shows the joint evolution of variance and MSE as a function of the time constant (TC). It is clearly observed that when TC increases from 10 to 30 min, the variance of the filtered power decreases significantly (from 3.5 to 1 W²), indicating better stability. However, this improvement is

accompanied by a gradual increase in the MSE (from 0.5 to 1.5 W²), indicating a loss of fidelity to the original signal. The remarkable point is at TC = 20 min, where the variance is halved (1.75 W²) while the MSE remains moderate (1 W²), confirming that this parameter offers the best compromise between stability and preservation of the photovoltaic signal characteristics. These quantitative results support the qualitative conclusions of the previous analyses.

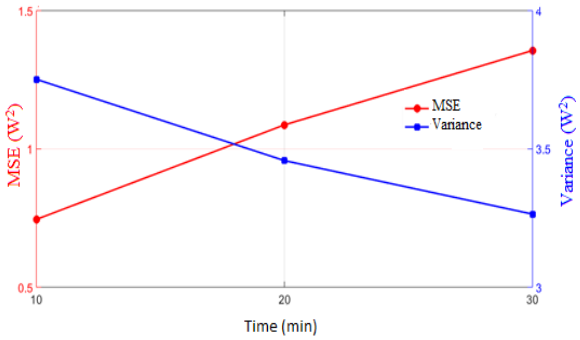

Fig. 11 – Joint evolution of MSE and variance

Figure 12 illustrates how the filtering degree affects the battery's demand differently. With TC = 10 min, the more frequent but moderate interventions (±600 W) produce many potentially underacted micro-cycles, resulting in an energy exchange of about 18 kWh. On the other hand, TC = 30 min results in fewer but more intensive interventions (±900 W), increasing the total energy converted to about 27 kWh. The ideal setting, TC = 20 min (±500 W), finds the right balance by simultaneously reducing the frequency and amplitude of requests, limiting the total energy converted to about 22 kWh, which validates its benefit for system durability. These findings highlight how crucial it is for PV systems to strike a balance between battery preservation and reactivity.

The thermal card for each TC's charge, discharge, and stable battery states is shown in Fig. 13. The version TC = 10 min exhibits a quick and disorganized change between states, which is indicative of a highly demanded battery to compensate for PV changes. With TC = 20 min, charge/discharge times become longer and more clearly defined, resulting in less abrupt transitions. In the case of TC = 30 min, there are longer stable phases along with more intensive charge/discharge periods. According to the analysis, TC = 20 min maximizes both the reduction of cycle stressors and the limiting of exchanged energy, extending the battery's lifespan.

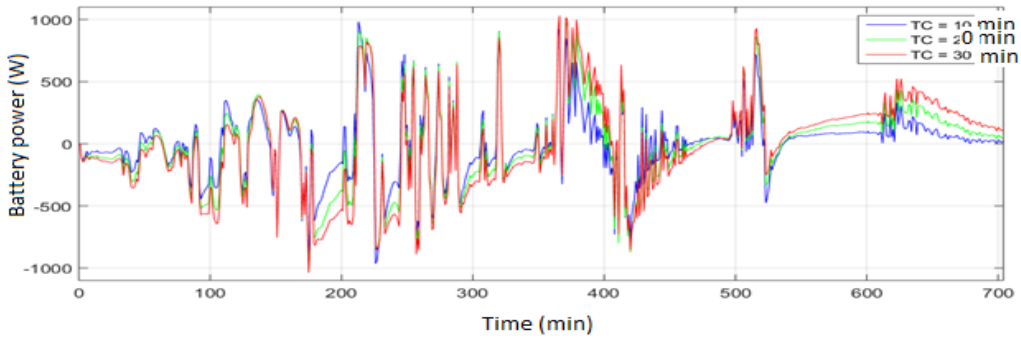

Fig. 12 – Battery charge/discharge profile

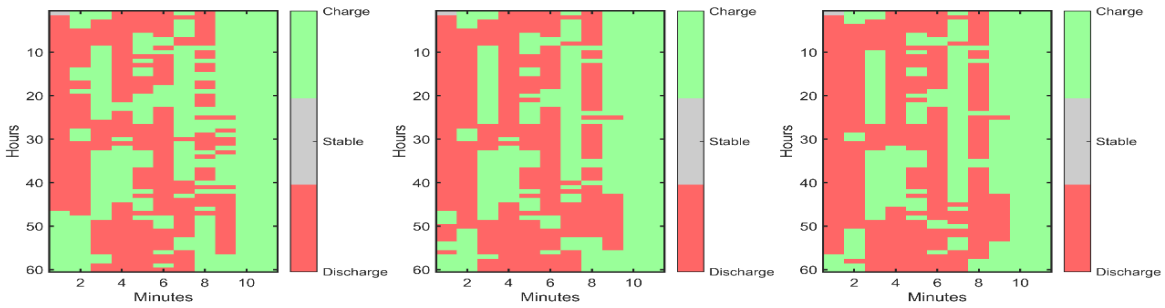

Fig. 13 – Charge /Discharge stable heat maps by TC

Figure 14 illustrates how the LPF filter affects the battery's state of charge (SoC) for various time constants (TC). The SoC exhibits frequent oscillations (78–86%) at TC = 10 min, indicating an excessive micro-cycle-induced solicitation. TC = 20 min provides an ideal profile with more consistent variations (80-85%), lowering stress while maintaining a margin of maneuver. On the other hand, TC=30min generates a trop plate curve (82–84%) that may conceal the system's actual requirements. These findings demonstrate that TC = 20 min is the optimal compromise, limiting both deep discharges and undesired cycles while maintaining the ability to respond to PV fluctuations. This analysis perfectly aligns with the findings of the other indicators that were examined.

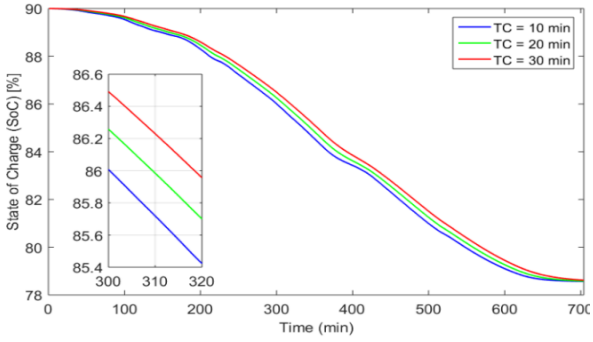

Fig. 14 – State of Charge evolution for each TC.

5. **CONCLUSION**

This study convincingly demonstrates that the discrete low-pass filter with a 20 min time constant represents the optimal compromise for grid-connected PV systems. By reducing fluctuations by 60% while limiting battery impact, this solution effectively addresses both grid stability and storage durability challenges.

Multivariate analyses (variance, MSE, RR%, SoC) and innovative SVM-based heatmap visualizations provide a clear, quantitative framework for energy managers to optimize smoothing parameters. Although centered on the CDER network, the methodology is reproducible for other climatic and grid contexts.

Future research should: (1) validate findings across diverse climatic zones; (2) integrate economic cost-benefit analysis (LCOS); (3) benchmark against real-time algorithms like adaptive Kalman filters or MPC using hardware-in-the-loop testing; and (4) incorporate chemistry-specific battery degradation models for accurate lifetime prediction. This contribution lays a solid foundation for optimal PV integration into modern electrical grids.

CREDIT AUTHORSHIP CONTRIBUTION STATEMENT

Saliha BOULAHCHICHE:methodology, data analysis, and writing.
Ismail BENDAAS: methodology, data analysis.
Smail SEMAOUI: data analysis, battery studies.
Amar HADJ ARAB: conceptualization, methodology, data analysis.
Kada BOUCHOUICHA, Abdelhak RAZAGUI, Kamel ABDELADIM: climate factor studies, data analysis

Received on 15 June 2025

REFERENCES

1. Y. Zhang, X. Li, H. Wang, *A hybrid energy storage system strategy for smoothing photovoltaic power fluctuation based on improved HHO-VMD*, International Journal of Photoenergy, 2023.
2. X. Wu, L. Chen, J. Liu, *An adaptive power smoothing approach based on artificial potential field for PV plant with hybrid energy storage system*, Solar Energy, **272**, pp. 112377 (2024).
3. M. Banjanin, M. Ikić, B. Perović, M. Milovanović, *Harmonic analysis of distributed energy sources using sliding FFT and IEC 61000-4-7*, Rev. Roum. Sci. Techn. – Électrotechn. et Énerg., **70**, *4*, pp. 507–512 (2025).
4. I.G. Dogaru, F.D. Dogaru, V. Năvrăpescu, L.M. Constantinescu, *From the photovoltaic effect to a low voltage photovoltaic grid challenge – a review*, Rev. Roum. Sci. Techn. – Électrotechn. et Énerg., **69**, *3* (2024).
5. S. Boulahchiche, A. Hadj Arab, S. Haddad, I. Bendaas, K. Bouchouicha, S. Bouchakour, S. Semaoui, A. Razagui, *Impact of a power ramp event on photovoltaic system power quality under different weather conditions and operating powers*, Electrical Engineering (2024).
6. S. Boulahchiche, A. Hadj Arab, S. Haddad, I. Bendaas, K. Bouchouicha, S. Bouchakour, S. Semaoui, A. Razagui, *Ramp rate control techniques to mitigate fluctuations in photovoltaic solar production*, Technological and Innovative Progress in Renewable Energy Systems, pp. 291–296, Springer (2025).
7. S. Boulahchiche, A. Hadj Arab, S. Haddad, I. Bendaas, A. Razagui, *Performance investigation of single-phase transformerless PV inverter connected to low voltage network*, Rev. Roum. Sci. Techn. – Électrotechn. et Énerg., **69**, *2* (2024).
8. S. Boulahchiche, A. Hadj Arab, S. Haddad, I. Bendaas, A. Razagui, *Power quality monitoring of rooftop photovoltaic penetration level on low voltage system*, 19th International Multi-Conference on Systems, Signals & Devices (SSD) (2022).
9. M.A. Syed, A.A. Abdalla, A. Al-Hamdi, M. Khalid, *Double moving average methodology for smoothing of solar power fluctuations with battery energy storage*, 2020 International Conference on Smart Grids and Energy Systems (SGES), pp. 291–296 (2020).
10. D. Benavides, P. Arévalo, E. Villa-Ávila, J.A. Aguado, F. Jurado, *Predictive power fluctuation mitigation in grid-connected PV systems with rapid response to EV charging stations*, Journal of Energy Storage, **86**, 111230 (2024).
11. P. Arévalo, D. Benavides, M. Tostado-Véliz, J.A. Aguado, F. Jurado, *Smart monitoring method for photovoltaic systems and failure control based on power smoothing techniques*, Renewable Energy, **205**, pp. 366–383 (2023).